International Conference on Mathematics and Computational Methods Applied to Nuclear Science and Engineering (M&C 2011)
Rio de Janeiro, RJ, Brazil, May 8-12, 2011, on CD-ROM, Latin American Section (LAS) / American Nuclear Society (ANS)
ISBN 978-85-63688-00-2

MODELING OF TUBE CURRENT MODULATION METHODS IN COMPUTED TOMOGRAPHY DOSE CALCULATIONS FOR ADULT AND PREGNANT PATIENTS

Peter F. Caracappa, and X. George Xu
Program of Nuclear Engineering and Engineering Physics
Rensselaer Polytechnic Institute, Troy, NY 12180-3590
caracp3@rpi.edu; xug2@rpi.edu

Jianwei Gu
GE Healthcare, Global Diagnostic X-ray
Waukesha, WI 53186
Jianwei.Gu@ge.com

ABSTRACT

The comparatively high dose and increasing frequency of computed tomography (CT) examinations have spurred the development of techniques for reducing radiation dose to imaging patients. Among these is the application of tube current modulation (TCM), which can be applied either longitudinally along the body or rotationally along the body, or both. Existing computational models for calculating dose from CT examinations do not include TCM techniques. Dose calculations using Monte Carlo methods have been previously prepared for constant-current rotational exposures at various positions along the body and for the principle exposure projections for several sets of computational phantoms, including adult male and female and pregnant patients. Dose calculations from CT scans with TCM are prepared by appropriately weighting the existing dose data. Longitudinal TCM doses can be obtained by weighting the dose at the z-axis scan position by the relative tube current at that position. Rotational TCM doses are weighted using the relative organ doses from the principle projections as a function of the current at the rotational angle. Significant dose reductions of 15% to 25% to fetal tissues are found from simulations of longitudinal TCM schemes to pregnant patients of different gestational ages. Weighting factors for each organ in rotational TCM schemes applied to adult male and female patients have also been found. As the application of TCM techniques becomes more prevalent, the need for including TCM in CT dose estimates will necessarily increase.

Key Words: Dosimetry, Computed Tomography, Tube Current Modulation.

1. INTRODUCTION

Radiation risk associated with routine or accidental patient exposure to x-ray computed tomography (CT) scans has become a headline topic in recent years [1]. Recent research has focused on methods to reduce CT dose to patients by employing a lower tube current without compromising image quality through automatic exposure control (AEC) that is based on the principle of tube current modulation (TCM) [2-4]. Such AEC systems are designed to adjust the tube current according to patient shape, size and x-ray attenuation characteristics. Existing AEC systems are generally based on two specific approaches: (1) longitudinal (or z-axis) AEC that modulates according to the patient body attenuation along the z-axis defined by a preliminary

localizer radiograph, and (2) “rotational” (or “angular,” or “x y-axis”) AEC that modulates during the rotational course to compensate for differences in attenuation between lateral and anterior-posterior projections [3-5]. The implementation of TCM differs among manufacturers and is very specific to the exam requirements and the patient.

Several studies have investigated the dose impact of TCM in specific situations. Angel et al. assessed the effects of TCM for modern multi-detector CT (MDCT) on breast doses using patient models developed from CT images [6]. Brisse et al. assessed the organ doses and effective doses for pediatric patients [7]. Since manufacturers do not provide details about the TCM algorithms, assumptions about the modulation schemes were made by the authors when reconstructing organ doses from procedures. The purpose of this study is to present generic methods for incorporating TCM into dose calculations.

2. METHODS AND MATERIALS

2.1. Dose Calculation Components

2.1.1. Patient phantoms

There are a wide range of computational models of the human body available for dose calculations. For this work, patient dose data was obtained using two sets of phantoms: the RPI-AM and RPI-AF phantoms representing normal adult patients, and the RPI P-series representing pregnant patients.

The RPI-AM and RPI-AF phantoms, seen in Figure 1(a), have more realistic anatomies as compared with the stylized MIRD-5 phantoms. Constructed using surface mesh data, the RPI adult phantoms consist of organs that have been deformed and adjusted in accordance with reference values recommended in the ICRP Report 89 [8]. For use in the Monte Carlo code, finalized mesh phantom was converted into voxels that were acceptable to the MCNPX code [9]. RPI-AM phantom consists of 24650750 (250 × 151 × 653) cubic voxels at 0.27 cm on each side, and RPI-AF phantom consists of 24466832 (247×151×656) cubic voxels at 0.25 cm on each side. In total, 28 different material compositions were defined and appropriately assigned to 122 separate organs or tissues for RPI-AM and 121 organs or tissues for RPI-AF. The organ elemental compositions and densities were derived from ICRP Publication 89 [8] and ICRU Report 46 [10].

The RPI P-series consists of realistic computational phantoms of a pregnant patient at the end of three gestational periods of 3, 6 and 9 months—called RPI-P3, RPI-P6 and RPI-P9 phantoms as illustrated in Figure 1(b)—have been previously developed [11]. Unlike partial-body CT images that contain limited number of organs defined by poor image quality [12], the RPI-P phantoms consist of organ volumes and masses carefully adjusted to agree with reference values recommended in the ICRP Publication 89 [8]. Since the phantoms representing the mother are adjusted to agree with the ICRP Publication 89, the body habitus is considered to be “normal,” representing a population average. The perimeter of the abdomen is 57 cm, 100 cm and 109 cm

for P3, P6 and P9 phantoms, respectively, which are different from the data set of the maternal perimeter provided by Angel et al. [12]. A total of 35 organs and tissues in the mother and fetus were included in these phantoms. The phantom geometries were designed with realistic representations of the fetus that includes the skeleton (except for the 3-month phantom), brain, and soft tissue. For Monte Carlo calculations, each phantom was voxelized at a resolution of 3 mm × 3 mm × 3 mm, involving a total of about 25 million voxels [13].

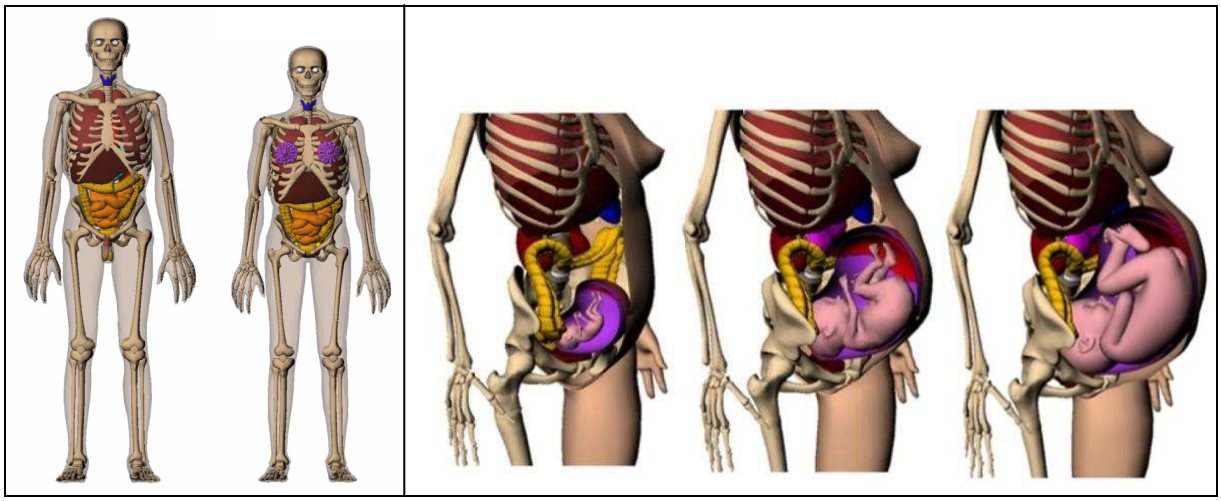

(a) (b)

Figure 1. Phantoms representing (a) adult male and female patients and (b) pregnant patients undergoing CT examinations

2.1.2. MDCT scanner model

Two MDCT scanner models for the GE LightSpeed Pro 16 and GE LightSpeedTM 16 (General Electric Healthcare Corporation, Waukesha, WI) were considered in this study to provide patient dose data for CT scans at various slab positions. The MDCT scanner models cover the energy spectrum, beam shape, bowtie filters, beam collimation as well as the source motion trajectory (i.e., helical path and pitch). The scanner models used for this study were validated with CTDI values using the method describe by Gu et al [14].

2.1.3. MCNPX simulations

All radiation transport and dose calculations were performed using the MCNPX Monte Carlo code [15]. MCNPX is a general purpose Monte Carlo radiation transport code that tracks all particles at all energies necessary for these simulations. Photon physics mode with the default energy cut-off was used. The photon transport model creates electrons but assumes that they travel in the direction of the primary photon and that the electron energy is deposited at the photon interaction site to satisfy the condition of charged particle equilibrium (CPE) [16], which is a valid assumption in the energy range of diagnostic x-rays. Under the conditions of CPE, the

collision kerma is equal to absorbed dose and is recorded using the type 6 (F6 : p) tally of the MCNPX. In all simulations, the number of histories was selected to achieve a relative statistical uncertainty of less than 5% in most organs (or detectors), and less than 10% for organs with the very small volumes or located at large distances from the primary beam.

2.2 Longitudinal Tube Current Modulation

In longitudinal tube current modulation, the current varies as a function of the slab position or z-axis position along the length of the body. The tube current value at a particular position is represented by *I(z)*, where *z* is the slab location. Simulated organ doses, *D(z)*, are available for each slab position normalized to a tube current of 100 mAs. Calculating the overall dose from a scan is a matter of finding the dose at each corresponding position along the z axis and weighting it appropriately by the tube current at that point. The total dose to a given organ from the scan is therefore given by

$$D = \int_{z_{min}}^{z_{max}} \frac{I(z)}{100 \text{ mAs}} D(z)\, dz \qquad (1)$$

An example of the longitudinal TCM is considered in application to pregnant patients. Three TCM protocols that had been applied to patients at Massachusetts General Hospital, Boston, at 15-week, 20-week and 31-week gestation, respectively, were adopted for this study. Although not an exact match of these gestational periods, the RPI-P3, P6 and P9 phantoms were used to represent these three patients. The slab locations corresponding to the starting and ending positions of the TCM scheme were found and matched to the RPI-P phantoms according to anatomical characteristics. For comparison, organ doses are also obtained for a non-TCM CT scan over the same range with a tube current corresponding to the maximum tube current used in the TCM scheme.

2.3 Rotational Tube Current Modulation

When TCM is accounted for in the rotational direction, the dose must be weighted by the tube current at a given source angle and the relative dose to the target organ at that source angle. Organ doses have previously been calculated for various photon energies from the six standard exposure directions: AP, PA, LLAT, RLAT, ROT, and ISO [9]. Although a CT exposure from a particular direction is not precisely equivalent to a wide-field parallel beam from the same direction as it is limited to the extent of the scan range, the effect on the organ dose will be similar if all or nearly the entire organ is included in the scan range.

As the x-ray source rotates around the body in a CT scan from 0 degrees through 360 degrees, it moves from the AP direction, through the LLAT, PA, and RLAT directions, returning back to the AP direction. At each of the four principle directions, the relative organ dose is known from the previous simulations. At intermediate angles, the differential dose is determined by a Pythagorean combination of the relative doses from the nearest two directions, by

$$\frac{dD}{d\theta} = \frac{I(\theta)}{\bar{I}} \sqrt{x^2 \cos^2\theta + y^2 \sin^2\theta} \tag{2}$$

where $I(\theta)$ is the tube current at angle θ, $\bar{I}$ is the average tube current for the rotation, and x and y represent the relative organ dose from the trailing and leading directions in the scan quadrant, respectively. For instance, Quadrant I, x would be AP and y would be LLAT, in Quadrant II, x would be LLAT and y would be PA, etc. For this case, the values of x and y are found by convolving the organ dose in each direction as a function of energy with the x-ray spectrum of the source (performing linear interpolation for x-ray energies between simulated photon energies), and normalizing to the organ dose in the AP direction. The total dose for the tube current modulated rotation is therefore given by:

$$D(z) = \bar{C} \sum_{Q=I}^{IV} \int_0^{\pi/2} \frac{dD}{d\theta} d\theta \tag{3}$$

The result is the dose for the rotation at the particular longitudinal position. The total dose for each organ will be found by integrating along the scan range in a manner similar to Equation (1).

3. RESULTS

3.1. Longitudinal Tube Current Modulation, Effects on Fetal Dose

The results of the sample longitudinal TCM scheme are presented in Table I, summarizing the calculated fetal doses for the three cases. For comparison, the fetal doses without TCM were also calculated at an mA equivalent to the maximum current in the TCM scheme for that case. The fetal doses from TCM are clearly smaller than those from non TCM in all cases. Furthermore, it was found that the fetal dose increased with the size of the fetus-a finding that is different from that of a previous study by Angel et al. [12]. This may be accounted for by the anatomical differences between the clinical cases and the patient phantoms used in this study.

3.2. Rotational Tube Current Modulation

The dose factors for each principle direction, representing the values of x and y for use in Equation (2), are presented in Table II. These values represent the dose factors for a 120 kVp x-ray source derived from the dose calculations for monoenergetic photon beams presented in [9].

Table I. Fetal doses calculated with and without the application of longitudinal tube current modulation

Organ	Organ dose (mGy)								
	Case 1			Case 2			Case 3		
	Non-TCM	TCM	Δ(%)	Non-TCM	TCM	Δ(%)	Non-TCM	TCM	Δ(%)
Fetal soft tissue	9.41	8.06	14.28	8.34	6.88	17.49	24.22	18.10	25.27
Fetal skeleton	NA[a]	NA[a]	NA[a]	27.52	22.83	17.06	67.19	50.26	25.19
Fetal brain	8.56	7.31	14.60	6.55	5.32	18.86	17.06	12.66	25.78
Fetus total	9.27	7.94	14.33	9.47	7.81	17.52	28.00	20.92	25.29

Table II. Relative Dose Factors for Internal Organs of RPI-AM and RPI-AF Phantoms for 120 kVp X-ray Beam

	Male				Female			
Organ	AP	PA	LLAT	RLAT	AP	PA	LLAT	RLAT
Brain	0.466	0.625	0.673	0.691	0.480	0.671	0.720	0.711
Breast	1.061	0.307	0.378	0.386	1.018	0.211	0.477	0.460
Colon	0.718	0.616	0.473	0.313	0.759	0.681	0.511	0.359
Eye lens	1.479	0.066	0.732	0.799	1.415	0.082	0.785	0.811
Gonads	1.349	1.075	0.216	0.214	0.889	0.541	0.244	0.256
Liver	1.035	0.379	0.203	0.595	0.941	0.491	0.297	0.606
Lung	0.908	0.752	0.348	0.370	0.754	0.846	0.389	0.453
Esophagus	0.814	0.491	0.486	0.476	0.770	0.593	0.335	0.395
Salivary Gland	0.573	0.540	0.878	0.769	0.751	0.304	0.763	0.730
Skin	0.945	0.943	0.636	0.632	0.961	0.949	0.668	0.669
Stomach	0.678	0.485	0.401	0.156	0.549	0.632	0.425	0.198
Thyroid	1.653	0.395	1.141	1.200	1.696	0.477	1.175	1.115
Bladder	0.766	0.744	0.180	0.187	0.843	0.849	0.236	0.220
Adrenals	0.179	1.408	0.203	0.183	0.200	1.219	0.271	0.269
Bone	1.797	1.855	1.107	1.118	1.876	1.810	1.208	1.217
ET Airways	1.072	0.164	0.667	0.649	1.006	0.194	0.696	0.673
Gall Bladder	0.727	0.398	0.217	0.268	0.693	0.423	0.271	0.343
Heart	1.106	0.358	0.437	0.346	0.892	0.439	0.530	0.341
Kidney	0.309	1.227	0.208	0.194	0.341	1.153	0.280	0.246
Lymph Nodes	0.906	0.655	0.371	0.369	1.005	0.540	0.364	0.449
Muscle	0.831	0.924	0.466	0.468	0.836	0.963	0.500	0.504
Oral Mucosa	0.725	0.272	0.809	0.826	0.770	0.338	0.905	0.878
Pancreas	0.338	0.999	0.340	0.055	0.349	1.012	0.393	0.078
Prostate/Uterus	0.747	1.033	0.157	0.164	0.925	0.592	0.313	0.304
Red Bone Marrow	0.794	1.035	0.478	0.480	0.828	1.110	0.535	0.540
Small Intestine	0.879	0.431	0.342	0.267	0.973	0.463	0.424	0.323
Spleen	0.602	0.762	0.870	0.039	0.655	0.776	0.891	0.057
Thymus	1.313	0.256	0.284	0.323	1.369	0.270	0.315	0.296

4. CONCLUSIONS

Tube current modulation methods have the potential to significantly reduce patient dose from CT examinations. Methods for finding patient dose from CT scans utilizing both longitudinal and rotational TCM schemes have been developed and demonstrated for various applications including normal adult patient and pregnant patient scans. As tube current modulation becomes a standard practice in radiology departments, methods such as these for incorporating TCM schemes in assessments of patient dose will be necessary.

ACKNOWLEDGMENTS

The authors would like to acknowledge Dr. Bob Liu of Massachusetts General Hospital for providing the TCM data used for the pregnant patients.

REFERENCES

1. W. Bogdanich, “Radiation Overdoses Point Up Dangers of CT Scans” *The New York Times* October 15, 2009.
2. S. M. Giacomuzzi, B. Erckert, T. Schopf, M. C. Freund, P. Springer, A. Dessl and W. Jaschke, "The smart-scan procedure of spiral computed tomograpy: a new method for dose reduction," *Rofo* **165**, 10-16 (1996).
3. M. Gies, K. W. A, W. H and S. C, "Dose reduction in CT by anatomically adpated tube current modulation. I. Simulation studies.," *Med. Phys.* **26**, 2235-2247 (1999).
4. W. A. Kalender, W. H and S. C, "Dose reduction in CT by anatomically adapted tube current modulation. II. Phantom measurements.," *Med. Phys.* **16**, 2248-2253 (1999).
5. N. Keat, "CT scanner automatic exposure control systems.," Medicines and Healthcare Products Regulatory Agency; ImPACT Report (2005).
6. E. Angel, N. Yaghmai, C. M. Jude, J. J. DeMarco, C. H. Cagnon, J. G. Goldin, A. N. Primak, D. M. Stevens, D. D. Cody, C. H. McCollough and M. F. McNitt-Gray, "Monte Carlo simulations to assess the effects of tube current modulation on breast dose for multidetector CT," *Phys. Med. Biol.* **54**, 497–511 (2009).
7. H. J. Brisse, M. Robilliard, A. Savignoni, N. Pierrat, G. Gaboriaud, Y. De Rycke, S. Neuenschwander, B. Aubert and J.-C. Rosenwald, "Assessment of Organ Absorbed Doses and Estimation of Effective Doses From Pediatric Anthropomorphic Phantom Measurements for Multi-Detector Row Ct With and Without Automatic Exposure Control," *Health Physics* **97**, 303-314 (2009).
8. ICRP-89, "Basic anatomical and physiological data for use in radiological protection: reference values," *Annals of the ICRP* **32**, 1-277 (2002).
9. J Zhang, Y Na, XG Xu “RPI-AM and RPI-AF, a pair of mesh-based, size-adjustable adult male and female computational phantoms using ICRP-89 parameters and their calculations for organ doses from monoenergetic photon beams” *Phys. Med. Biol.* **54** 5885-908 (2009).
10. International Commission on Radiation Units and Measurements (ICRU) “Photon, electron, proton and neutron interaction data for body tissues” *ICRU Report 46.* Bethesda, Md., USA (1992).

11. X. G. Xu, V. Taranenko, J. Zhang and C. Shi, "A boundary-representation method for designing whole-body radiation dosimetry models: pregnant females at the ends of three gestational periods—RPI-P3, -P6 and -P9," *Phys. Med. Biol*. **52**, 7023-7044 (2007).
12. E. Angel, C. V. Wellnitz, M. M. Goodsitt, N. Yaghmai, J. J. DeMarco, C. H. Cagnon, J. W. Sayre, D. D. Cody, D. M. Stevens, A. N. Primak, C. H. McCollough and M. F. McNitt-Gray, "Radiation Dose to the Fetus for Pregnant Patients Undergoing Multidetector CT Imaging: Monte Carlo Simulations Estimating Fetal Dose for a Range of Gestational Age and Patient Size," *Radiology* **249**, 220-227 (2008).
13. V. Taranenko, J. Zhang, D. Zhang, X. G. Xu and C. Shi, “Preliminary External Dosimetry Data from a New Set of Mother/Fetus Models” *Transactions of the American Nuclear Society* **96,** 448 (2007).
14. J. Gu, B. Bednarz, P. F. Caracappa and X. G. Xu, "The development, validation and application of a multi-detector CT (MDCT) scanner model for assessing organ doses to the pregnant patient and the fetus using Monte Carlo simulations," *Phys. Med. Biol*. **54**, 2699-2717 (2009).
15. D. B. Pelowitz, "MCNPXTM USER’S MANUAL Version 2.5.0," (2005).
16. J. J. DeMarco, C. H. Cagnon, D. D. Cody, D. M. Stevens, C. H. McCollough, J. O'Daniel and M. F. McNitt-Gray, "A Monte Carlo based method to estimate radiation dose from multidetector CT (MDCT): cylindrical and anthropomorphic phantoms," *Phys. Med. Biol*. **50**, 3989-4004 (2005).